POAC'17
Busan, KOREA

Proceedings of the 24th International Conference on
Port and Ocean Engineering under Arctic Conditions
June 11-16, 2017, Busan, Korea

A Parametric Study on Turning Ability of Icebreaking Ships in Level Ice

Donghyeong Ko[1], Kyung-Duk Park[1], Youngjae Sung[1]
Hyundai Heavy Industries Co., Ltd

ABSTRACT

A parametric study is carried out to determine major design parameters in turning ability of ice breaking vessels in level ice. Turning ability in ice is becoming an important part of ship design along with the interest in ice resistance. Thus, HHI developed the time-domain simulation to analyze turning ability of the icebreaking ships. This simulation considers icebreaking process and pattern induced by the ice-hull interactions. The usefulness of the scheme was validated by the application of a few bow-first icebreaking models (Ko et al. 2016). In this study, the application of the simulation is extended to various icebreaking models including conventional twin-screw ship and pod-driven ships. To understand which design parameter of icebreaking ships is dominant on turning ability, the effects of length-breadth ratio, rudder area ratio, stem angle and shoulder angle on ship design parameters were studied through many numerical simulations.

KEY WORDS: Turning ability, Icebreaking ships, Pod-driven ships, Twin-screw ships

INTRODUCTION

HHI has designed several icebreaking ships during the arctic projects to meet the growing demand for the natural resource transportation through the northern sea route. In the early stage of icebreaking ship design, the ship performance, such as speed and manoeuvrability in level ice is mostly considered because these items are directly related to owner's requirement.

The ship performance of icebreaking ships is influenced by the interaction between ship and ice. To understand the ship-ice interaction, the mechanism for icebreaking in level ice divides into three parts: breaking, buoyancy, clearing by many researchers (Shimanskii, 1938; Enkvist, 1972; Inonov, 1981; Lindqvist, 1989). The researchers also suggested a couple of empirical formulas based on principal hull dimension, such as length, breadth, depth, stem angle around waterline, etc. The formulas give a certain level of accuracy, but the formulas cannot reasonably reflect the detailed design variation of candidate hull forms which have different design characteristics despite same principal dimension. For this reason, HHI developed the new ice resistance prediction program which is based on modified empirical formulas to take hull form variation into account (Park et al., 2015). The method showed some improvement in estimation of ice resistance for icebreaking ships. However, because

the method cannot handle yaw moment and side force on the hull, it has a limit to estimating turning ability in level ice.

Biao Su (2011) has introduced semi-empirical time domain simulation to understand the icebreaking performance of small sized ice breakers in level ice. In the simulation, breaking process is numerically considered by adopting crushing-bending failure while buoyancy and clearing parts are computed by the empirical formula of Lindqvist (1989). This method well represents the icebreaking patterns and the turning ability, and it shows good agreement with full scale measurements for an icebreaker by Riska et al. (2001).

HHI has suggested modified semi-empirical time domain simulation for icebreaking commercial vessels which has long parallel middle body. (Ko et al., 2016) To release excessive ice loads on the long parallel middle body, they proposed varying crushing stress which is varied according to the velocity vector and theoretical curve of Ashby et al. (1986). For the simulation of ship motions, the modular type mathematical model with multiple pod propulsors (Kim et al., 2006) was used. The simulation results are compared with the model tests.

In this study, the application of HHI's modified semi-empirical time domain simulation is extended to various icebreaking models including conventional twin-screw ship and pod-driven ship. To understand which design parameter of icebreaking ships is dominant on turning ability in level ice, the effects of length-breadth ratio, rudder area ratio, stem angle at bow and flare angle at shoulder on ship design parameters were studied through many numerical simulations.

NUMERICAL SIMULATION

Procedure

Basic procedure of the modified semi-empirical time domain simulation is derived from the Biao Su's thesis (2011). Among the ice induced force by ship-ice interaction, breaking component is numerically simulated and the other ones (buoyancy and clearing components) are simply computed from Lindqvist's empirical formula (1989).

The flow chart of the numerical simulation is briefly summarized in figure 1. The detailed procedures were also described in the paper of Ko et al. (2016). At first, it is assumed that a ship moves ahead in the level ice with given initial conditions, such as dimension of the ship, hydrodynamic coefficient in open water, propeller open water characteristic and ice data. As the ship goes on, it detects contact areas around the hull at each time step. If the contact area was found, the code checks crushing-bending failure and calculates the force and yaw moment acting on the ship. After the bending failure occurs, then ice nodes are regenerated.

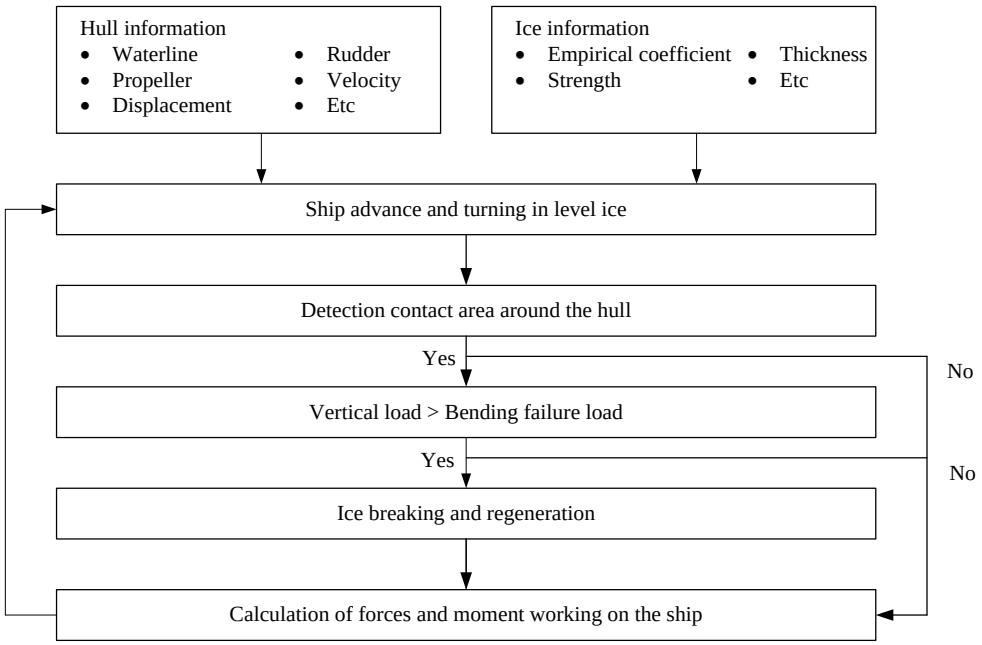

Figure 1. Flow chart of numerical simulation

Varying crushing stress

This procedure adopts a new concept of varying crushing stress. The new concept considers the influence of the contact area and the direction of impact due to a ship-ice interaction. If the ship and ice are fully crushed, crushing stress normal to the contact area is generated. According to Ashby et al. (1986), the crushing stress σ_{area} can be defined as a function of contact area A as follows.

$$\sigma_{\text{area}} = \frac{P}{A} = \frac{P_L \Delta_L}{L_i^3}\left[1 + 3\left(\frac{L_i^3}{A\Delta_L}\right)^{\frac{1}{2}}\right] \quad (1)$$

where, L_i is an idealized size of cubical independent cells, Δ_L is a moved distance before the cell fails and P_L is the average force during the period of contact.

On the other hand, the Eq. (1) shows that the stress extremely soars as contact area decreases. Thus, for small contact area, the varying crushing stress curve is bounded by the experimental results of the maximum stress, 10.5 MPa to avoid the unrealistic situation. (Sanderson, 2014) The overall crushing stress curve is described in figure 2.

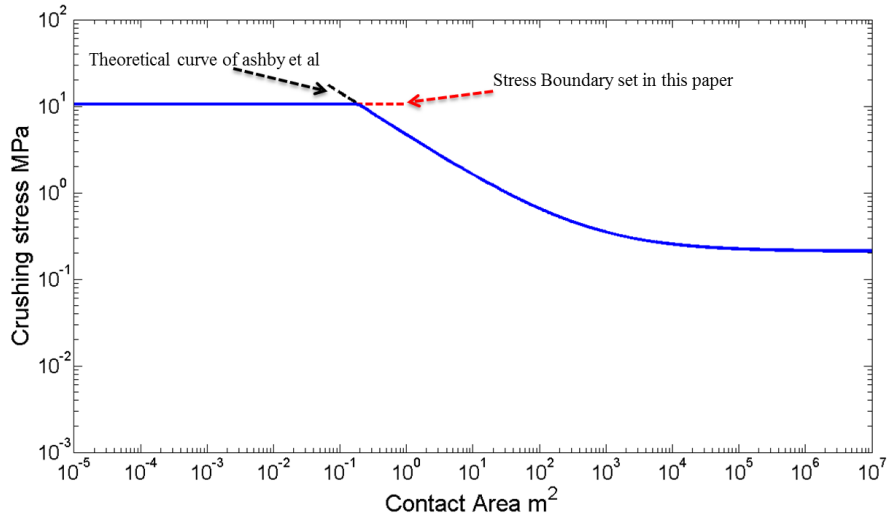

Figure 2. Theoretical curve of Ashby et al. (1986) bounded by the collected data

The relation between the direction of advancing ship and the direction of the crushing force defined by the contact area is also considered as well as the varying crushing stress. If the ship crushes the ice diagonally, due to the direction of ship advance, the ice is not fully crushed. To implement this effect, the velocity vector of the ship is newly considered. Velocity vector of ship ($\vec{U}$) is assumed to comprise of two components, linear velocity ($\overrightarrow{U_l}$) and angular velocity ($\overrightarrow{U_r}$) and defined as

$$\vec{U} = \overrightarrow{U_l} + \overrightarrow{U_r} \tag{2}$$

Once the contact areas are determined, the resulting crushing stress is calculated according to the curve in figure 2 and divided into two components: normal and vertical to the ice sheet, considering the slope angles between hull and ice such as α and β in figure 3. Then, vertical crushing stress σ_v and normal crushing stress σ_n are generated as the ship contacts ice. However, they are zero if the ship moves far from the ice although such a contact between hull and ice happens. Therefore, the resulting crushing stresses are given as in Eq.s (3) and (4), where the normal stress is the cosine α component and the vertical stress is the cosine β component of σ_{area}.

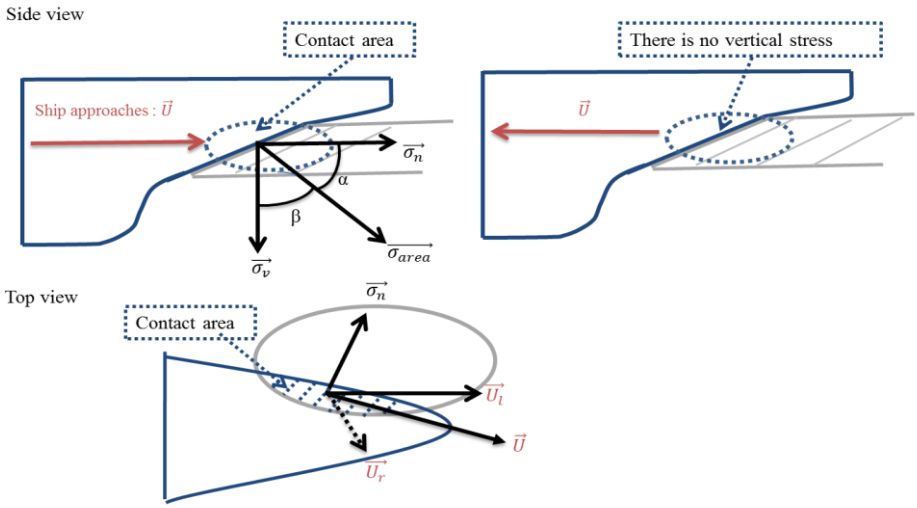

Figure 3. Description of contact area and crushing stress

$$\sigma_n = \sigma_{area} \cdot t_1 \cdot \cos\alpha$$
$$\sigma_v = \sigma_{area} \cdot t_2 \cdot \cos\beta \tag{3}$$

$$t_1 = \begin{cases} \frac{\vec{U}\cdot\overrightarrow{\sigma_n}}{|\vec{U}|\cdot|\overrightarrow{\sigma_n}|} & if \ \frac{\vec{U}\cdot\overrightarrow{\sigma_n}}{|\vec{U}|\cdot|\overrightarrow{\sigma_n}|} > 0 \\ 0 & if \ \frac{\vec{U}\cdot\overrightarrow{\sigma_n}}{|\vec{U}|\cdot|\overrightarrow{\sigma_n}|} \leq 0 \end{cases}$$

$$t_2 = \begin{cases} 1 & if \ \frac{\vec{U}\cdot\overrightarrow{\sigma_n}}{|\vec{U}|\cdot|\overrightarrow{\sigma_n}|} > 0 \\ 0 & if \ \frac{\vec{U}\cdot\overrightarrow{\sigma_n}}{|\vec{U}|\cdot|\overrightarrow{\sigma_n}|} \leq 0 \end{cases} \tag{4}$$

In Eq. (4), t_1 and t_2 represent the effect of the ship advance and their values are determined according to the inner product between velocity vector ($\vec{U}$) and inward normal vector of ice sheet ($\overrightarrow{\sigma_n}$).

Simulation of ship performance based on modular model

In the study, the modular type mathematical model is and two different types of ships are considered for the simulation. One is a pod-driven ship which has three pod propulsors and the other is a conventional twin-screw ship. This mathematical model is based on twin pod propulsor model (Kim et al., 2006), and then slightly modified for the pod-driven ship and twin-screw ship. Right-handed coordinate system with Z vertically downward is used and its origin is located at the center of gravity. Prior to the simulation, by the Newton's second law, the ship's equations of motion (u, v, r) can be described in Eq. (5).

$$M \cdot (\dot{u} - vr) = X_H + X_P + X_R + X_{ice}$$
$$M \cdot (\dot{v} + ur) = Y_H + X_P + Y_R + Y_{ice} \tag{5}$$
$$I_{zz} \cdot \dot{r} = N_H + N_P + N_R + N_{ice}$$

The terms (X, Y and N) with subscript (H, P, R, ice) represent the forces and yaw moment acting on hull induced by hydrodynamic effect, propeller (or pod propeller), rudder (or pod struts) and ice respectively. Prior to the simulation, the test results from open water propeller test and PMM (Planar Motion Mechanism) tests were conducted for icebreakers to obtain relative coefficient induced by propeller hydrodynamic effect.

Derivatives of hydrodynamic effect are introduced below.

$$\begin{aligned} X_H &= -M_x\dot{u} + \left(M_y + X_{vr}\right)\cdot vr + X_{vv}\cdot v^2 + X_{rr}\cdot r^2 + X(u) \\ Y_H &= -M_y\dot{v} + Y_v\cdot v + Y_{vvv}\cdot v^3 + Y_r\cdot r + Y_{rrr}\cdot r^3 + Y_{vrr}\cdot vr^2 + Y_{rvv}\cdot rv^2 \\ N_H &= -J_{zz}\cdot\dot{r} + N_v\cdot v + N_{vvv}\cdot v^3 + N_r\cdot r + N_{rrr}\cdot r^3 + N_{vrr}\cdot vr^2 + N_{rvv}\cdot rv^2 \end{aligned} \quad (6)$$

Forces and moment induced by propeller (pod propellers) and rudders (or pod struts) are formulated in Eq. (7) and (8) respectively.

$$\begin{aligned} X_P &= (1-t)(T^P + T^C + T^S)\cos\delta_p \\ Y_P &= (1-t)(T^P + T^C + T^S)\sin\delta_p \\ N_P &= x_p\cdot(1-t)(T^P + T^C + T^S)\sin\delta_p - y_p\cdot(1-t)(T^P - T^S)\cos\delta_p \end{aligned} \quad (7)$$

$$\begin{aligned} X_R &= -(1-t_R)(F_N^P + F_N^C + F_N^S)\sin\delta_r \\ Y_R &= (1+a_H)(F_N^P + F_N^C + F_N^S)\cos\delta_r \\ N_R &= (x_R + a_H x_H)(F_N^P + F_N^C + F_N^S)\cos\delta_r - y_R\cdot(1-t_R)(F_N^P - F_N^S)\sin\delta_r \end{aligned} \quad (8)$$

where, *P, C, S* (port, center, starboard) represent the location of each device.

In the equation, δ_p and δ_r mean turning angle of propeller and rudder respectively. Since the twin-screw ship has two stationary propellers (δ_p=0), rudder is assumed to be a single device for the ship manoeuvering.

SIMULATION RESULTS

Comparison with Model Tests

In the design phase, various ship designs are compared for the decision-making. There are a few ways to determine optimum design of a ship, such as experience-based design, numerical simulation and model test. For the non-ice class ships, experience-based design is useful approach in the early phase. Accumulated data from a number of model tests and sea trial tests help to evaluate maneuverability of the ship in a relatively short period of time. For icebreaking ships, however, experience-based design is inadequate due to the lack of data. Although the model test is the most accurate method, a lot of time and cost are needed to refreeze the ice repeatedly.

On the other hand, there is no restriction in cost and time required for numerical simulation. Even if the uncertainty of numerical simulation is much more than model test, its cost and time are cheaper and shorter. Thus, if we have a numerical simulation which corresponds with the model test result it will be a good alternative for the small design change.

In this study, the model tests for two different types of mother ships are compared with their numerical simulations before a parametric study. The principal dimensions of the ships and ice model test conditions are summarized in table 1. The model ships are tested in the same ice condition but they have slightly different slenderness ratio and bow angle. The ships tested in the ice model basin are presented in figure 4.

Table 1. Principal dimension of ships and ice model test conditions

	Pod-driven ship	Twin screw ship
L/B	5.5	5.6
Bow angle (degree)	20	25
Ice thickness (m)	1.7	1.7
Flexural strength (kPa)	500	500
Propulsion unit	Azipod	Propeller
Number of propulsion unit	3	2

Figure 4. Stern of the model ships (Pod-driven ship: Top, Twin-screw ship: Bottom)

Comparison results between the simulation and model tests are shown in table 2. The full turning diameter of model tests is extrapolated from initial turning track because ice model basin has long and relatively narrow channel in general. The resulting mean velocity and turning diameter from the numerical simulations well agree with the model tests for both types of ships. From the turning ability point of view, the most distinctive characteristic of the pod-driven ship is that pod body is able to rotate for turning and this makes the thrust force generate additional yaw moment directly. For this reason, pod-driven ship has a great advantage in its turning ability. This tendency is shown in both model tests and numerical simulations. Dimensionless turning diameter (Turning diameter / Length) of the both ships are significantly different. In the model tests, dimensionless turning diameter of the Twin screw ship marked 112 but the pod-driven ship 34. For reference, turning tracks of both simulations and model tests are shown in figure 5 and figure 6 respectively.

Table 2. Turning data from model test and numerical simulation

	Mean velocity [m /s]	Turning diameter [Turing diameter / L]
Pod-driven ship [model test]	0.4	33.6
Pod driven ship [simulation]	0.5	33.3
Twin-screw ship [model test]	1.2	112.1
Twin-screw ship [simulation]	1.3	103.4

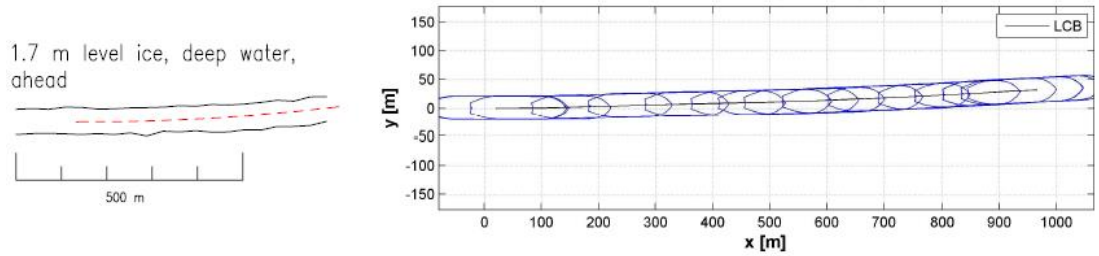

Figure 5. Turning tracks of the model tests (Pod-driven ship: Left, Twin-screw ship: Right)

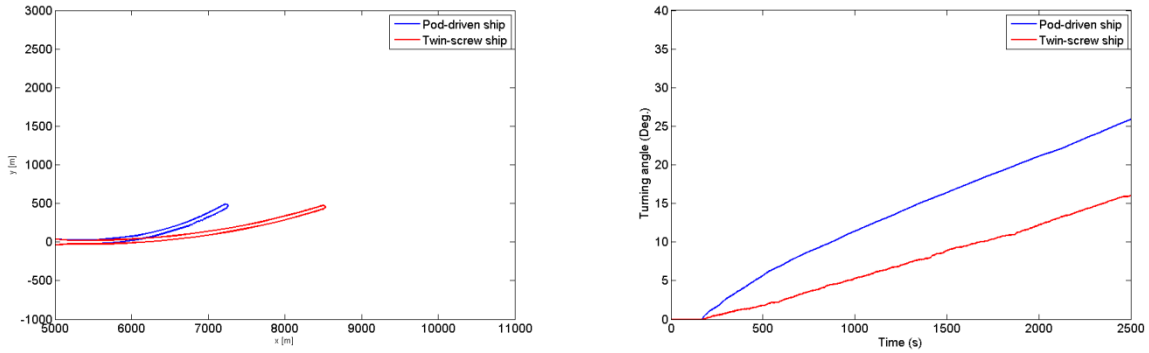

Figure 6. Turning track and angle of the numerical simulations

Parametric Study

For many decades, many different kinds of ships has been tested to verify their turning ability in open water. Through the tests, it was found that some significant dimensionless coefficients related to the turning ability were C_bB/L (C_b: block coefficient, B: Breadth, L: Length), A/LT (A: rudder area, L: length, T: depth), stem angle at bow region and flare angle at shoulder region. Higher C_bB/L normally has an influence on the smaller turning diameter. Also, higher A/LT (rudder area ratio) has same characteristic as C_bB/L.

For dimensionless coefficients, numerical simulations are conducted to monitor what the turning ability in level ice is like. In the study, some design parameters such as slenderness, block coefficient and rudder area are changed to check which parameter of a ship is dominant on the turning ability. Figure 7 shows the tendency of the dimensionless turning diameter with respect to slenderness ratio (B/L). Turning diameter decreases as the ratio increases regardless of types of ships and this tendency is similar to open water test result. As a result, slender ship is unfavorable to turning ability in ice as it is in open water. In addition, the impact of block coefficient (C_b) is studied in figure 8. In general, C_b is directly related to inertial mass as a factor of course stability in open water turning ability. However, parallel shifts are observed with the change of C_b in the simulation in level ice. This indicates C_b has no effect on the turning ability in level ice. In other words, the effect of ice induced force is much larger than that of the inertial mass induced by C_b variation for turning ability.

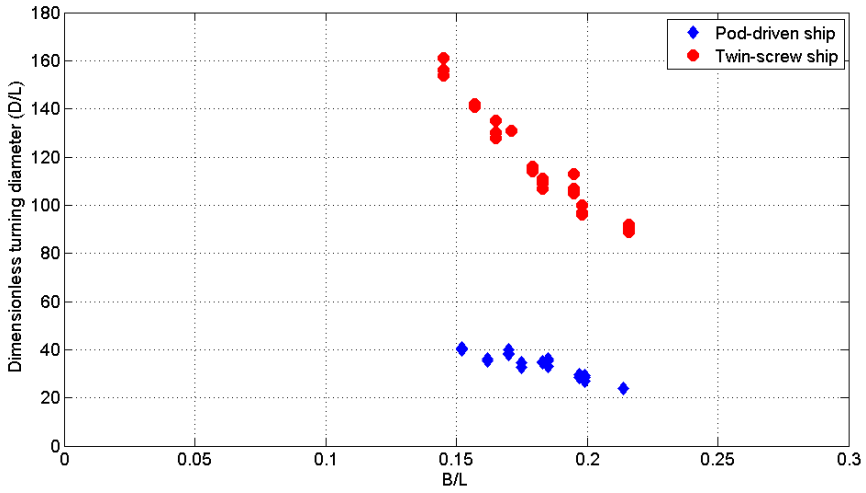

Figure 7. Dimensionless turning diameter with respect to slenderness ratio (B/L)

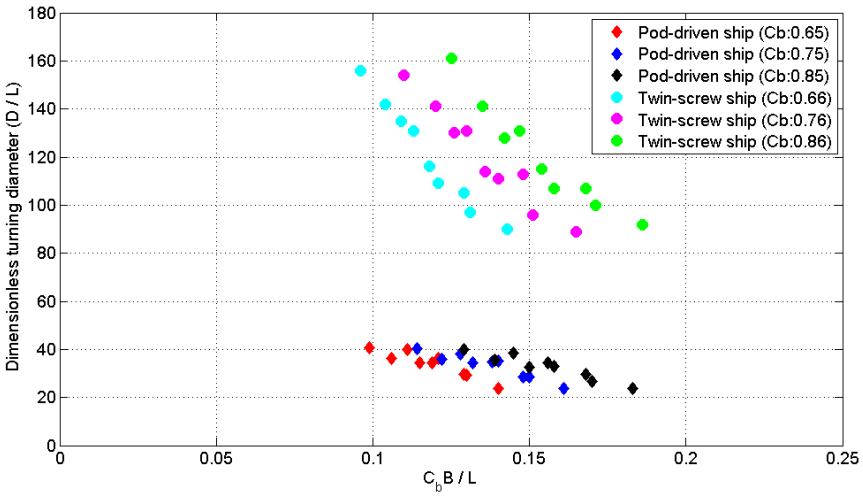

Figure 8. Dimensionless turning diameter with respect to C_bB/L

The rudder area ratio effect in turning ability was studied. Length and rudder area of the ships altered to see the aspect of the relationship between the rudder area ratio and turning diameter. Figure 9 indicates that rudder area ratio effectively impacts on the turning diameter for both ships but the gradient is rather different. Since pod propeller is turning along with the pod strut, pod propeller activates as an auxiliary device for ship manoeuvering. On the other hand, twin-screw ship has conventional propeller-rudder system. In the system, rudder only acts as a manoeuvering device. For that reason, variation of the rudder area ratio directly affects the gradient of the turning diameter on the twin-screw ship. The gradient of the twin-screw ship is approximately 4 times larger than the pod-driven ship.

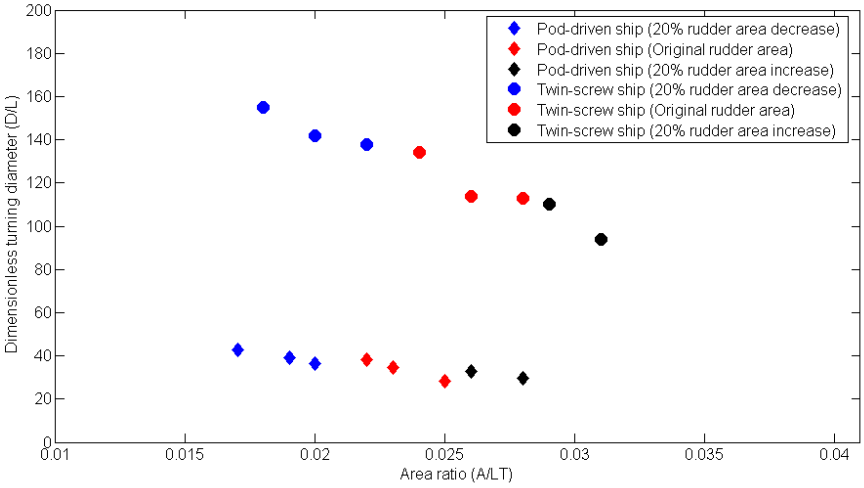

Figure 9. Dimensionless turning diameter with respect to rudder area ratio (A/LT)

To see the impact of hull form variation on the turning ability, stem angles at bow region and flare angles at shoulder region are changed in the simulation. The meaning of bow region and shoulder region illustrates in figure 10. Bow region is defined from the position of

forward perpendicular to a width of 0.1 B. In addition, shoulder region is within the region not exceeding 0.1 B from the start position of parallel middle body.

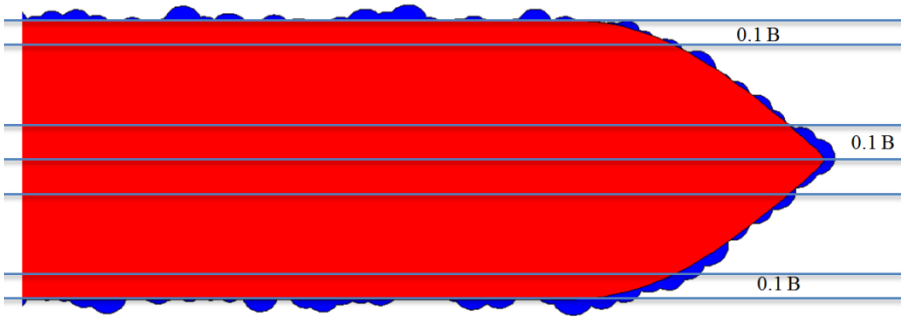

Figure 10. Definition of bow and flare region

For both ships, stem angle variation at bow region was studied. The relation between turning diameter and stem angle is represented in figure 11. With reduced stem angles, turning ability in level ice is not noticeably improved. Reduced stem angle helps to relieve the stress level at bow region and it makes the average velocity of the ships increase as shown in table 3. Thus, it is thought that the increased ship velocity leads to slightly bad turning ability in level ice. On the other hand, ~~However,~~ the direction of crushing force at bow region is almost aligned with the x-axis and thus the crushing stress variation with nearly zero moment arm do not much contributed to the turning ability in level ice.

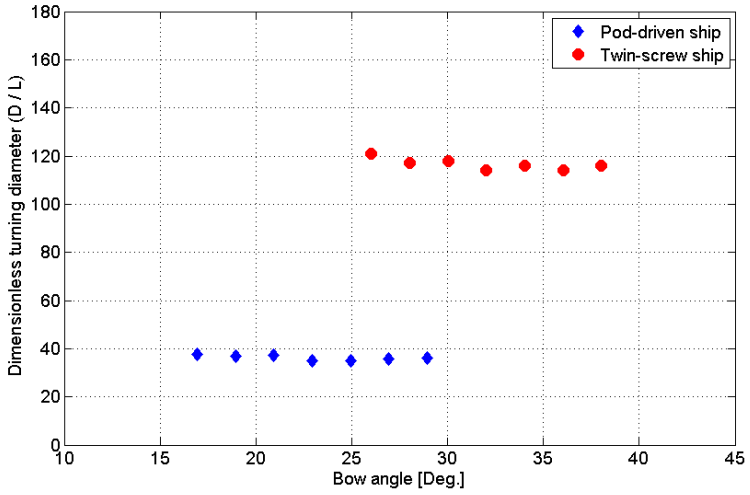

Figure 11. Dimensionless turning diameter with respect to bow angle

Table 3. Average velocity and yaw rate of both ships *(In this table, velocity ratio and yaw rate ratio are represented by the ratio of the corresponding model to reference model.)*

Stem angle variation	Velocity ratio (Pod-driven)	Velocity ratio (Twin-screw)	Yaw rate ratio (Pod-driven)	Yaw rate ratio (Twin-screw)
Model 1(-6 degree)	111.4 %	103.5 %	104.9%	103.6%
Model 2(-4 degree)	107.5 %	101.5 %	108.4%	98.9%
Model 3(-2 degree)	103.7 %	101.1 %	99.1%	101.3%
Original ship (reference point)	100.0 %	100.0 %	100.0%	100.0%
Model 4(+2 degree)	98.1 %	97.6 %	101.6%	98.7%
Model 5(+4 degree)	94.1 %	98.5 %	99.4%	106.7%
Model 6(+6 degree)	93.6 %	97.9 %	93.8%	100.4%

Flare angle variation at the shoulder part of a ship is also studied. Figure 12 shows the effect of flare angle variation about turning diameter in level ice. With reduced flare angles, the turning ability is conspicuously improved in level ice. By contrast with the stem angle variation, the variation of crushing occurred at the shoulder area affect the yaw moment of a ship because of relatively long moment arm.

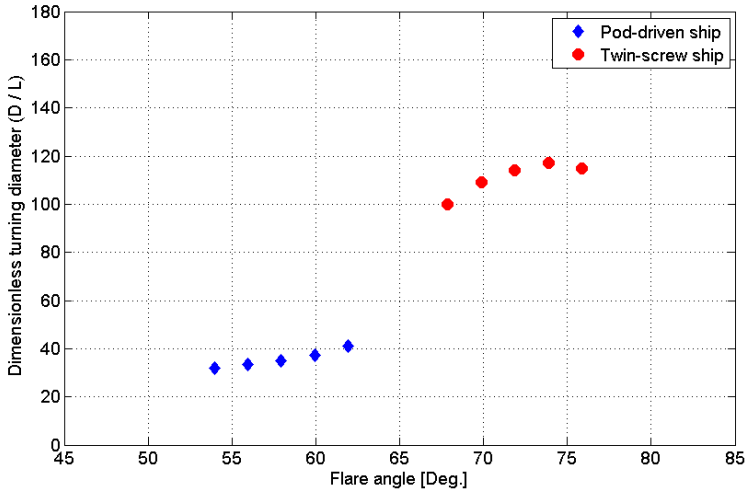

Figure 12. Dimensionless turning diameter with respect to flare angle

CONCLUSIONS

Using the modified semi-empirical time domain simulation, a parametric study is carried out to find out what design parameters of ice breaking vessels are dominant on turning ability in level ice. Prior to a parametric study, comparison study between numerical simulation and model test for pod-driven and twin-screw models is conducted to see the usefulness for the simulation technique suggested in this study. Tendency of dimensionless turning diameter is monitored with variation of ship design parameters, such as slenderness ratio, block coefficient, rudder area ratio, stem angle at bow and flare angle at shoulder. The results of the parametric study are summarized as follows.

- Slenderness ratio is quite related to the turning ability in level ice as with in open water. Higher slenderness is a bad influence on the turning ability in ice.
- While block coefficient normally affects the turning ability in open water, it doesn't in level ice because the effect of ice induced force is much larger than the inertial mass.
- Higher rudder area ratio is helpful for small radius of turning trajectory. This effect emerged as a key parameter in twin-screw ship. However, it is less remarkable for pod-driven ship because pod strut is not a main device for turning.
- Flare angle variation at shoulder region is much more related to the turning ability compared with stem angle at bow for both ships. In bow region, crushing stress generally acts on the ship in the same direction of x-axis. Thus, crushing stress around the bow region do not much contributes to the yaw moment in the simulation. On the other hand, acting point of crushing force around the shoulder region has relatively long moment arm and it is an effective uptake to increase yaw moment.

Even though this study enables us to analyze some features of turning ability in level ice, there are two typical shortcomings in the simulation. First, there is no guarantee that the breaking patterns estimated by this simulation correspond well with that of model tests. Second, both buoyancy and clearing components are estimated by using Lindqvist's empirical formula suggested to calculate ice resistance in x direction only and thus this formula does not reflect an additional influence on yaw moment in practice. It means that turning operation in level ice leads to the unbalanced flow patterns of the fractured ices on the sides of a ship after icebreaking process, and thus it needs to be considered to include secondary effect due to the unbalanced buoyancy and clearing forces. These problems will be dealt with in future works.

REFERENCES

Ashby, M.F., Palmer,A.C., Thouless, M., Goodman, D.J., Howard, M.W., Hallam, S.D., Murrell, S.A.F., Jones, N., Sanderson, T.J.O. and Ponter, A.R.S, 1986. Nonsimultaneous failure and ice loads on Arctic structures. Offshore Technology Conference 1986 NO. OTC 5127, pp. 399-404, Houston, USA.

Enkvist, E., 1972. On the Ice Resistance Encountered by Ships Operating in the Continuous Mode of Icebreaking. Report No.24, The Swedish Academy of Engineering Science in Finlande, Helsinki, Finland.

Izumiyama, K., Wako, D., Shimoda, H. and Uto, S., 2005. Ice load measurement on a model ship hull. Proceedings of 18TH International Conference on Port and Ocean Engineering under Arctic Conditions (POAC), New York, USA.

Ko, D.H, Park, K.D., Ahn, K.S., 2016. Time domain simulation for icebreaking and turning capability of bow-first icebreaking models in level ice. International Journal of Naval Architecture and Ocean Engineering. Vol. 8, Issue 3, pp 228-234

Park, K.D. and Kim, H.S., 2014. Study on the Ship Ice Resistance Estimation Using Empirical Formulas. Proceedings of the ASME 2014 33rd International Conference on Ocean, Offshore and Arctic Engineering (OMAE), San Francisco, USA.

Lindqvist, G., 1989. A straightforward method for calclation of ice resistance of ships. Proceedings of 10th International Conference on Port and Ocean Engineering under Arctic Conditions (POAC), Lulea, Sweden.

Riska, K.,Leiviska, T., Nyman, T., Fransson, L.,Lehtonen, J., Eronen, H. and Backman, A.,2001. Ice Performance of the Swedish Multi-Purpose Icebreaker Tor Viking Ⅱ. Proceedings of PAC 2001, pp.849-865.

Sanderson T.J.O, 2014, Ice Mechanics. Springer, Lexington, USA.

Schneider, P.J. and Eberly, D.H., 2002. Geometric Tools for Computer Graphics. Morgan Kaufmann Publishers, San Francisco, USA.

Shimanskii, Y.A., 1938. Conditional standards of ice qualities of a ship. Trans. Arctic Research Institute, Northern Sea Route Administration Publishing House, Vol. 130, Leningrad. Translation T-381-01 by Engineering Consulting and Translation Center (ECTC), P.O. Box 1377, Jackson Heights, New York, NY 11372.

Su, B, 2011. Numerical Predictions of Global and Local Ice Loads on Ships. PH.D. Thesis. Department of Marine Technology, Norwegian University of Science and Technology, Norway.

Yeon-gyu K., Sunyoung K., Youngha P., Byeongseok Y. and Sukwon L., Prediction of Maneuverability of a Ship with POD Propulsion System. Journal of the Society of Naval Architects of Korea Vol. 43, No. 2, pp. 164-170